Journal of Applied Electrochemistry **32**: 1219–1227, 2002.

An approximate solution to the model of a sparged packed bed electrode reactor

Y. SUN[1], B. WU[1], O. QIU[1], W. XU[1] and K. SCOTT[2,*]
[1]*Taiyman University of Technology, Taiyuan 030024*
[2]*Department of Chemical and Process Engineering, University of Newcastle upon Tyne, Newcastle, NE1 7RU*
*(*author for correspondence, e-mail: k.scott@ncl.ac.uk)*

Received 25 April 2000; accepted in revised form 16 July 2002

Key words: anodic oxidation, gas–liquid reactor, inverse operator method, nonlinear mathematical model, propylene oxide

Abstract

An approximate analytical solution to the mathematical model of a sparged packed bed electrochemical reactor (SPBER) in which a gaseous reactant undergoes direct anodic oxidation is presented. The model is based on two strongly nonlinear partial differential equations and is solved by the inverse operator method (IOM). The solution is used to study the direct anodic oxidation of propylene. The approximate IOM solution is useful in that it enables the direct investigation of the effect of model parameters on the operation of the reactor. Current density against electrode potential, polarization data, for the anodic oxidation of propylene in the SPBER is presented. Nonlinear parameter estimate methods are used to fit the model to experimental data to obtain physically meaningful values of kinetic parameters.

List of symbols

a_l	gas–liquid interfacial area (m^{-1})
a_p	specific surface area of electrode (m^{-1})
C_{AB}	concentration of OH^- in the bulk solution (kmol m^{-3})
$C_{AB,s}$	concentration of OH^- on the electrode surface (kmol m^{-3})
C_{gi}	concentration of species i in the bulk gas (kmol m^{-3})
C_i	concentration of species i in the bulk solution (kmol m^{-3})
C_{is}	concentration of species i on the electrode surface (kmol m^{-3})
D_{rl}	lateral effective diffusivity of OH^- (m^2 s^{-1})
D_i	diffusion coefficient of species i (m^2 s^{-1})
D_p	diameter of particle (m)
D_b	diameter of bubble (m)
e	packed bed void fraction
F	faradaic constant (96 500 C mol^{-1})
i	current density (A m^{-2})
i_0	exchange current density (A m^{-2})
I	observed current (A)
k_l	operating overpotential at membrane (V)
k_f	electrochemical reaction rate constant (m s^{-1})
k	mass transport coefficient (m s^{-1})
k_{li}	gas–liquid mass transport coefficient (m s^{-1})
m_i	phase distribution coefficient
PP	propylene
PG	propylene glycol
PO	propylene oxide
R	gas constant (J mol^{-1} K)
r_i	reaction rate (kmol m^{-3} s)
r_i^a	rate of gas absorption (kmol m^{-3} s)
S	electrode surface (m^2)
u_g	speed of gas bubble (m s^{-1})
u_l	speed of liquid (m s^{-1})
ΔU	null potential (V)
w	thickness of anodic (m)

Greek symbols

α	transfer coefficient
η	overpotential (V)
σ	specific conductivity (S m^{-1})
ϕ	potential (V)
ε_g	gas void fraction
τ	holding time of gas (s)
ρ_I	density (kg m^{-3})
μ	viscosity (Pa s)

1. Introduction

A mathematical model of a sieve plate gas–liquid electrochemical reactor (SPER) [1], which accounted for the mass transport processes occurring at the electrode–electrolyte interface, where chemical reactions also occur, and at the gas–liquid interface, has previously been applied to the indirect oxidation of propylene to propylene oxide using anodically generated halogen.

This reaction has been the subject of quite detailed modelling, by Alkire and Lisius [2] and Scott [3], the focus of which was to determine the reaction rate distribution in the solution phase.

The oxidation of alkenes has attracted significant interest over recent decades as a potentially attractive route for organic electrosynthesis [4]. This has included attempts to carry out the reaction, selectively, by direct anodic oxidation to eliminate problems associated with the *in situ* use of electrochemically generated oxidants. Recent studies have thus reported the direct oxidation of propylene to propylene oxide on stainless steel electrodes in alkaline solution [5, 6]. This process was also carried out in undivided cells, in which hydrogen gas is produced, at the cathode, in conjunction with the epoxide, at the anode. The disadvantage of an undivided cell is that the hydrogen gas reduces the partial pressure of propylene, which has a low solubility in the electrolyte, and thus imposes practical limitations on the degree of conversion of the propylene in the gas phase. Separation of propylene, hydrogen and propylene oxide (and water vapour mixtures) represents a significantly large cost to the process. This disadvantage, coupled with the relatively high effective electrolyte resistance, due to a high volume fraction of gas in the interelectrode gap, made the use of a packed bed electrochemical reactor, with propylene oxidation separated from the generation of hydrogen gas, a potentially attractive alternative synthesis method. Packed bed electrode reactors have important advantages over conventional electrochemical reactors for reactions with slow rate or with low reactant concentrations, that is, they provide a large electrode surface area per unit of reactor volume and provide very good mass transport conditions.

In the design and optimization of a process involving a sparged packed bed electrochemical reactor (SPBER) it is useful to model the performance of the reactor. Based on elemental principles of electrochemical reaction engineering, the lateral distributions of potential, current density and concentration in a SPBER are studied in this paper. A mathematical model that accounts for the electrochemical and chemical kinetics and mass transport is developed. This model can be solved by a numerical method based on a finite difference routine, For example, BAND(J) [7]. However, it is often more convenient for studying the behaviour of electrochemical reactors, to acquire an approximate analytical solution of the model because the relationship between the behaviour of the reactor and various parameters is then clearer and is more easily tested by experiment. It is well known that acquiring an approximate analytical solution of a nonlinear differential equation is difficult and a good approximate solution method and especially for strongly nonlinear differential equations, has not been available.

In the 1980s a method for the solution of nonlinear differential equation, the inverse operator method (IOM), was developed by Adomian [8]. This is an active field in nonlinear science that is particularly useful in studying nonlinear problems. It has been proved, by mathematical theory and application, that the IOM can solve strong nonlinear differential equations without hypotheses such a linearity, perturbation *etc*. [9].

This paper reports the use of the IOM to study the problem in electrochemical reaction engineering of the distribution of current density, electrode potential and concentration in a multiphase packed bed reactor. The strong nonlinear model of a SPBER is solved by IOM and an approximate analytical solution is used to investigate the effect of model parameters on the operation of the reactor. Current density–potential curves for the anodic oxidation of propylene in the reactor are presented and nonlinear parameter estimate methods are used to fit the model to experimental data to obtain physically meaningful parameter values.

2. Theoretical model

2.1. *Reaction kinetics for the direct anodic oxidation of propylene*

We consider here the electrochemical kinetics of the anodic oxidation of propylene in alkaline media. This reaction has been studied by Chou and Chang [5] who, within the range of parameters studied, determined that the reaction was zero order in propylene and first order in hydroxide ion concentration. Anodic oxidation is believed to take place by a reaction path involving the formation and adsorption of oxy or hydroxyl species, on the electrode surface, which, in the presence of propylene, produce the epoxide. The overall anodic reaction is

$$2OH^- + C_3H_6 \rightarrow C_3H_6O + H_2O + 2e^- \tag{1}$$

At high overpotentials the electrode kinetics can be represented by the following high field Butler–Volmer approximation:

$$i = 2i_o \frac{C_{AS}}{C_{AS,0}} \exp\left(\frac{\alpha_a F}{RT}\eta\right) \tag{2}$$

where $C_{AS,0}$ is the equilibrium concentration of OH^- ion at the electrode surface at the equilibrium potential. $C_{AS,0} = 1.0$ mol dm^{-3} in this case.

Introducing the influence of mass transport of OH^- ion at the electrode, with a mass transfer coefficient, k we obtain

$$i = \frac{C_{AB}}{\dfrac{1}{\dfrac{2i_o}{C_{AS,0}}\exp\left(\dfrac{\alpha_a F}{RT}\eta\right)} + \dfrac{1}{k_s}} \tag{3}$$

where $k_s = nFk$ and C_{AB} is the concentration in the bulk solution. The model ignores the occurrence of secondary reactions such as oxygen evolution at the anode.

The final kinetic rate equation developed by Chou and Chang [5] is quoted as

$$i = C_{AB} \exp\left[\frac{-(11.8 - 0.194F\eta)}{RT}\right] \tag{4}$$

2.2. *Reactor model for SPBER*

In a SPBER, for reactant to reach the electrode surface the reactant must diffuse across the gas–liquid interface, through the liquid film into the main body of liquid, and then through the mass transfer boundary layer (diffusion film) at the electrode. At the surface of the electrode, reactants are electrochemically converted to product according to appropriate electrochemical kinetics. The configuration of a SPBER, in which gas and electrolyte are introduced separately into the packed bed anode chamber, separated from the cathode chamber by a diaphragm or membrane, is shown schematically in Figure 1.

The assumptions used in the model are as follows: (i) the packed bed can be treated as a differential bed; (ii) in the packed bed the only important gradients are those normal to the fluid flow; (iii) the potential of the electrode phase has a constant value due to the high conductivity of the electrode phase compared to that of the electrolyte phase; (iv) the electrolyte entering the reactor is saturated with propylene; and (v) steady-state and isothermal operation.

The secondary, hydrolysis, reaction of propylene oxide to propylene glycol is only significant at high pH, and at high concentrations [5]. With the condition that this reaction in solution is neglected, then the distributions of overpotential, η and concentration of hydroxide ion in the bulk solution of the SPBER, C_{AB} are given by

$$\frac{d^2\eta}{d^2x} - \frac{a_p i}{\sigma} = 0 \tag{5}$$

$$D_{rl}\frac{d^2C_{AB}}{d^2x} - 2r_l = 0 \tag{6}$$

$$r_i = a_p i/2F \tag{7}$$

where D_{rl} is the diffusivity of hydroxide ion in the solution.

Substituting Equation 3 into Equations 5 and 6 gives the following model equations:

$$\frac{d^2\eta}{dx^2} - \frac{a_p}{\sigma}\frac{C_{AB}}{(C_{AS,0}/2i_o)\exp\left(\frac{\alpha_a F}{RT}\eta\right) + \frac{1}{k_s}} = 0 \tag{8}$$

$$D_{rl}\frac{d^2C_{AB}}{dx^2} - \frac{a_p}{F}\frac{C_{AB}}{(C_{AS,0}/2i_o)\exp\left(\frac{\alpha_a F}{RT}\eta\right) + \frac{1}{k_s}} = 0 \tag{9}$$

The boundary conditions for Equations 8 and 9 are:

$$x = 0, \quad \eta = \text{constant} = k_1, \quad C_{AB} = \text{constant} = k_2 \tag{10, 11}$$

$$x = w, \quad \frac{dC_{AB}}{dx} = 0 \tag{12}$$

The model presented in this paper can be solved by using the central finite difference method. Newman [7] outlines a suitable procedure BAND(J), for expressing the ordinary differential equations in finite difference form. Because the model is nonlinear, it is necessary to put the nonlinear equation in linear form and iterate over the nonlinearities. Bennion's subroutine DIFEQ [10], which can handle all the linearization and details associated with calling BAND(J), is used.

2.3. *Solution of reactor model by IOM*

Adomian developed a decomposition method to solve a range of nonlinear differential equations [8]. The method is applied in the solution of the reactor model in this work to obtain an appropriate analytical solution. The Adomian method is summarized in the Appendix.

Solving this reactor model, by IOM, the distributions of overpotential and hydroxide ion concentration are obtained as follows:

$$\eta = Y + k_1 + \Psi_1 \tag{13}$$

$$C_{AB} = \frac{B_2}{A_1 B_1}Y + k_2 + \Psi_2 \tag{14}$$

The accuracy of the Adomian method depends upon the number of polynomials used in the solution of the model. Using high orders (>3) is generally complex and can lead to slow convergence of solution. Hence the expression for Y is determined from a third order Adomian polynomial as

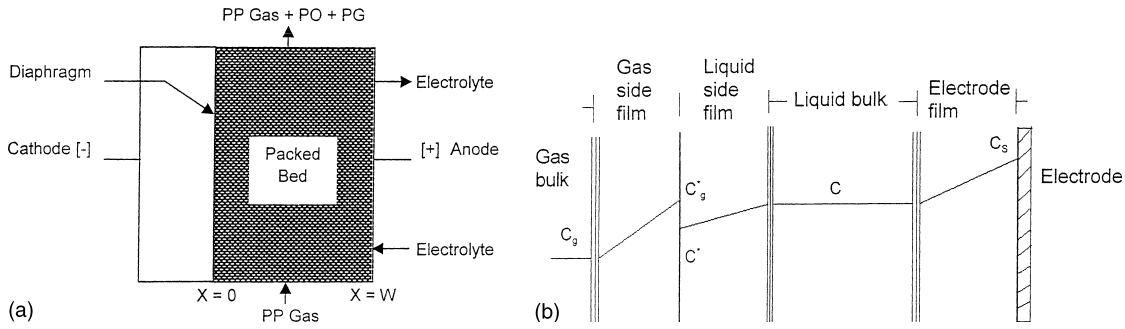

Fig. 1. (a) Schematic diagram of sparged packed bed reactor and (b) three-phase reaction.

$$Y = k_2 a \frac{x^2}{2} + \frac{k_2 a^2 \beta}{24} + \left(\frac{k_2 a^3 \gamma}{120} + \frac{k_2 a^3 \beta^2}{720}\right) x^6 + \frac{k_2 a^4 \beta \gamma}{6960} x^8 + \frac{k_2^2 a^4 \beta \gamma}{64\,800} x^{10} + \frac{k_2^2 a^5 \gamma^2}{918\,720} x^{12} \quad (15)$$

and the coefficients of Y are given by the following expressions:

$$a = \frac{A_1 A_2}{b} \exp(A_3 k_1) \quad (16)$$

$$b = A_2 A_4 \exp(A_3 k_1) + 1 \quad (17)$$

$$\beta = \frac{B_2}{A_1 B_1} + \frac{k_2 A_3}{b} \quad (18)$$

$$\gamma = \frac{k_2 A_3^2}{b}\left(\frac{1}{b} + \frac{1}{2}\right) + \frac{A_3 B_2}{b A_1 B_1} \quad (19)$$

$$A_1 = \frac{a_p}{\sigma},\ A_2 = 2i_o, \quad A_3 = \frac{\alpha_a F}{RT},\ A_4 = 1/k_s \quad (20)$$

$$B_1 = D_{rl},\ B_2 = \frac{a_p}{F} \quad (21)$$

With a constant operating overpotential k_1, the integrals of η, and C_{AB} from $x = 0$ to $x = w$, are given as

$$\overline{\eta(k_1)} = \int_0^w \eta(x)\mathrm{d}x/w \quad (22)$$

$$\overline{C_{AB}(k_1)} = \int_0^w C_{AB}(x)\mathrm{d}x/w \quad (23)$$

By substituting Equations 22 and 23 into the electrode kinetic Equation 3, and multiplying by the anode area S, the approximate analytical solution for the operating current, in terms of overpotential and other parameters, is obtained as

$$I(k_1) = iS = \frac{\overline{C_{AB}(k_1)S}}{\dfrac{C_{AS,0}}{2i_o \exp\left(\dfrac{\alpha_a F}{RT}\right)\overline{\eta(k_1)}} + \dfrac{1}{k_s}} \quad (24)$$

3. Effect of parameters on the behaviour of reactor

Gas sparging affects both the potential distribution and mass transport processes. The potential distribution is influenced by the effective conductivity of the electrolyte which depends on the fraction of gas in the two phase mixture. The effect of gas void fraction on the effective conductivity can be expressed by, for example, the following Bruggeman equation [11]:

$$\sigma/\sigma_0 = (1 - \varepsilon_g)^{1.5} \quad (25)$$

The effect of gas sparging on the mass transport process in the reactor can be described by the following empirical equations [12–16]:

(a) The gas void fraction is expressed as a function of the gas velocity:

$$\varepsilon_g = 0.62(U_g \mu_l/\sigma_l)^{0.575}(\mu_l^4 g/\rho_l \sigma_l)^{-0.131} \times (\rho_g/\rho_l)^{0.062}(\mu_g/\mu_l)^{0.107} \quad (26)$$

(b) For the gas–liquid mass transport coefficient:

$$10^3 k_l \varepsilon/U_l = 7.96[(-\Delta\rho/\Delta L)g\varepsilon/a_p \rho_l U_l]^{0.275} - 9.41 \quad (27)$$

(c) For the liquid–solid mass transport coefficient:

$$Sh/Sh_o = 1 + 4\mathrm{Re}_g^{0.55}\mathrm{Re}_l^{-0.7},\ \text{where } Sh = kd_h/D_i \quad (28)$$

$$d_h = \varepsilon d_p/[1.5(1 - \varepsilon)]$$

$$Re_l > 10, \quad Sh_o = 0.75\, Re_l^{0.5}\, Sc^{0.33}$$

(d) For the lateral dispersion coefficient:

$$Pe = 17.5\, Re^{0.75} + 11.4 \quad (29)$$

$$0.4 < Re < 500$$

The parameters used in the simulation are given in Table 3. The objective of the simulation of the model is to study the lateral distributions in overpotential, current density and concentration in the packed bed electrode under various operating conditions so that the reactor performance can be optimized.

Consider now the effect of parameters on the behaviour of SPBER. The exchange current density, i_0, is an important parameter in electrode kinetics and is a measure of the freedom from kinetic limitations. A reaction with a large value of i_0 is frequently said to be '*fast*' or '*reversible*'. The effect of i_0 on the behaviour of the reactor is shown in Figure 2. When the value of operating overpotential is small (<50 mV), the reaction rate is kinetically controlled and i_0 has an important influence on the operating current of the reactor. The larger the value if i_0, the larger is the value of operating current in the reactor. As the operating current increases, the effect of i_0 on the operating current become weaker and, eventually, at large operating overpotentials, the reactor is controlled by mass transport. It should be stressed here that the value of i_0 is apparently very large and reflects the difficulty in obtaining the equilibrium potential in this reaction system. The values selected are based on the value determined from the work of Chou and Chang [5].

An important parameter that affects the behaviour of SPBER is the gas sparging rate of propylene as this has a significant influence on both the reaction rate and mass transport rate. It is shown in Figure 3, that there is

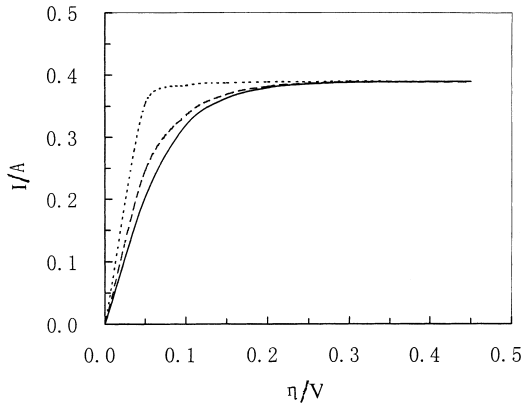

Fig. 2. Effect of exchange current density i_0 on the operating current I for the SPBER. $k = 1.01 \times 10^{-3}$ ms^{-1}, $\alpha = 0.35$. Other conditions as Table 1. i_0: (—) 1000, (- - -) 2500 and (···) 5000 A m^{-2}.

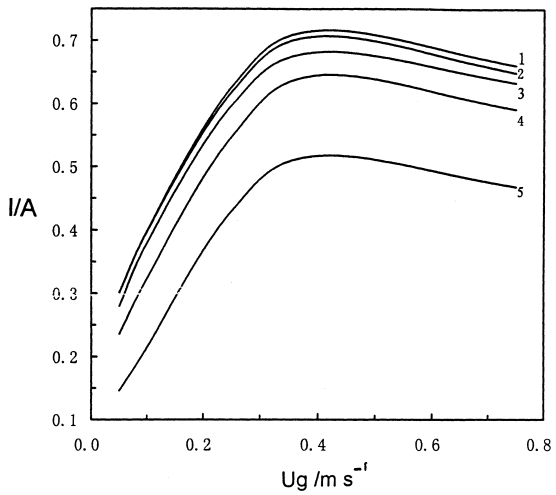

Fig. 3. Effect of gas velocity on the operating current I. $\alpha = 0.38$, $i_0 = 1.2 \times 10^4$ A m^{-2}. Overpotential k_1: (1) 0.25, (2) 0.2, (3) 0.15, (4) 0.1 and (5) 0.05 V.

an 'optimum' value of the gas sparging velocity at which a maximum in current is attained, at a particular cell overpotential. In this data, as the value of gas velocity increases, from 0.01 m s^{-1}, the operating current increases rapidly due to an increase in mass transport. When the value of gas velocity exceeds 0.25 m s^{-1}, the rate of increase in current density slows. This is because the gas void fraction increases which decreases the effective electrolyte conductivity thus reducing the depth of penetration of current into the packed bed reactor. As the value of gas velocity increases further (0.75 m s^{-1}), the current falls due to the large gas void fraction.

4. Experimental details

4.1. *Experimental apparatus*

The working electrode (anode) is a packed bed electrode made from 120 mesh stainless steel screen (68.7% Fe, 9.3% Cr, 10.1% Ni, 1.8% Mn, 0.07% C, 0.1% others). The width of the packed bed electrode is 3.0 cm. The counter electrode is a stainless steel sheet for hydrogen evolution. The anode and cathode are separated by an asbestos diaphragm to prevent mixing of the hydrogen gas with the propylene product gas. Reactant gas is fed into the cell via a gas distributor positioned at the base of the cell.

4.2. *Experimental procedure*

Prior to electrolysis the electrodes are pretreated in the following way. The electrodes are dipped into an 1.0 M KOH solution for approximately 0.5 h and then washed with distilled water. The electrodes are then introduced into the cell and polarized for 10 min. The electrolyte solutions are prepared from distilled water and C.P. grade KOH. In operation only two thirds of the cell is filled with the electrolyte solution, to provide space above the solution for foam separation. The temperature of operation is controlled by immersing the cell in a water bath. The gas sparging rate is controlled by a soap film flowmeter. The parameters of the cell are given in Table 1.

Before the start of an experiment the electrolyte is bubbled with propylene, for about 15 min, to purge oxygen, and other impurities, and to saturate the electrolyte before a constant overpotential is applied to the cell. The I/V relationship for the anodic reaction is measured by a potentiostat, model 363 (EG & G PAR) using a saturated calomel reference electrode. The null potential (i.e., the open-circuit potential between the working electrode and the reference electrode) ΔU_b is recorded every 10 min. When the null potential is constant, the measurements are started with the gas sparging rate kept constant. The potential $E(E = k_{1+\phi_{re}} + U_{\Delta b})$ at the membrane is changed stepwise and the current is recorded at each steady potential (after approximately 10 min). The I/V relationships at varying gas sparging rates are then measured successively.

4.3. *Experimental results*

Figure 4. shows experimentally determined steady-state current as a function of applied overpotential at three gas sparging rates. The null potential, ΔU_b under various operating conditions is constant at $\Delta U_b = 0.2$ V. The current increases with potential as expected and, at the higher gas velocities, exhibits a limiting, mass transport controlled, current. At very large potentials

Table 1. Experimental system parameters

Anode area	5.0 m^2
Anode thickness	0.03 m
Electrolyte volume	1.0 m^3
Electrolyte concentration	0.1 kmol m^3
Electrolyte conductivity	2.5 Ω^{-1} m^{-1}
Electrolyte temperature	298.15 K

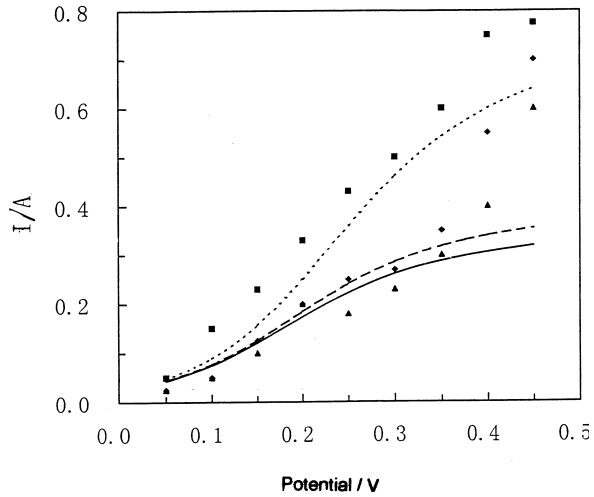

Fig. 4. Experimental steady state cell current electrode potential behaviour. Key: (—) $u_g = 0.05$ m s^{-1}, $\sigma = 1.56$ S m^{-1}; (- - -) $u_g = 0.1$ m s^{-1}, $\sigma = 1.92$ S m^{-1}; and (···) $u_g = 0.25$ m s^{-1}, $\sigma = 2.1$ S m^{-1}.

the current rises again with potential, which is probably a result of the secondary, oxygen evolution, reaction. At low gas velocity, when mass transport conditions are not good, a limiting current is not apparent. The solid lines in Figure 4 are model predictions which are discussed below. Agreement between the model and predicted values is reasonable up to electrode potentials of around 0.35 V. At higher potentials the model predictions deviate from experimental values due to the absence of a large well defined limiting current region in the oxidation reaction, that is, oxygen evolution becomes a significant secondary reaction. This lack of agreement between model and experiment is not considered critical as a major objective of the model is to provide a convenient and relatively simple means of estimating parameters for the SPBER.

4.4. *Nonlinear parameter estimates*

The model of the SPBER, presented above, depends on, amongst other things, the parameters i_0, α_a and k_s. These parameters can be obtained by independent experiment, if available, or determined by applying nonlinear parameter estimation [17] to the model and experimental data. In the case of a gas–liquid–solid electrochemical system there is great difficulty in measuring electrochemical kinetics and mass transport parameters by independent experiments and so nonlinear parameter estimation is a suitable method. The parameters, can be regressed from the experimental data (such as operating current), which is obtained relatively easily.

As a nonlinear parameter estimation method, the nonlinear least squares regression (NLS) is used. The NLS consists of minimising the following nonlinear objective function:

$$F(\beta) = \sum \varepsilon^2 = \sum (I - \hat{I})^2 \tag{30}$$

where $\hat{I}$ is given by Equation 27 at the experimental conditions. The computation necessary to minimise the objective function become more complicated with a nonlinear function; however there are computer programmes which can perform the necessary calculation (e.g., in reference [18]). The regression results of the model parameters are shown in Table 3 and residual values are shown in Table 4.

Table 2 also presents a comparison of the NLS parameter estimates with literature values [5]. The values of k_s are the same order of magnitude as values in the literature [19] and are considered to be representative of conditions in the reactor. The values of transfer coefficient, α_a, are larger, approximately twice, the literature values whilst the values of exchange current density, i_0 are smaller than those of literature. The experimental and estimated exchange current density values are of a similar order of magnitude which is considered reasonable. The difference in electrochemical kinetic parameters may be attributed to the difference in electrode material used in this study and in previous experimental work [5]. In particular the value of exchange current density is very sensitive to material type, morphology and also pre-treatment. In the case of the transfer coefficient the literature value was obtained for a three dimensional electrode for which current distribution theory [20] predicts that the Tafel slope is twice that measured for a planar, two-dimensional electrode, that is, the transfer coefficient is half the expected value for a planar electrode. Thus the model parameter estimate to transfer coefficient, which is applicable to a planar electrode, would be expected to be twice that of the literature value.

Figure 5 shows the typical variation of current density and overpotential in the reactor as predicted by the model. The data reflect the higher activity of the reactor closer to the diaphragm. As the current has to penetrate further into the packed bed from the diaphragm the current density and overpotential fall.

Figure 6 shows a comparison of predicted overpotential against current density behaviour, using IOM, with

Table 2. Values of the nonlinear parameters

u_g/m s^{-1}	i_0/A m^{-2}	Literature i_0/A m^{-2}	α_a	Literature α_a	k_s/m s^{-1}	Literature k/m s^{-1}
0.05	8.7×10^4		0.466		5.47×10^{-4}	3.84×10^{-4}
0.10	8.0×10^4	4.2×10^5	0.468	0.22	6.01×10^{-4}	5.04×10^{-4}
0.25	7.0×10^4		0.419		7.19×10^{-4}	7.54×10^{-4}

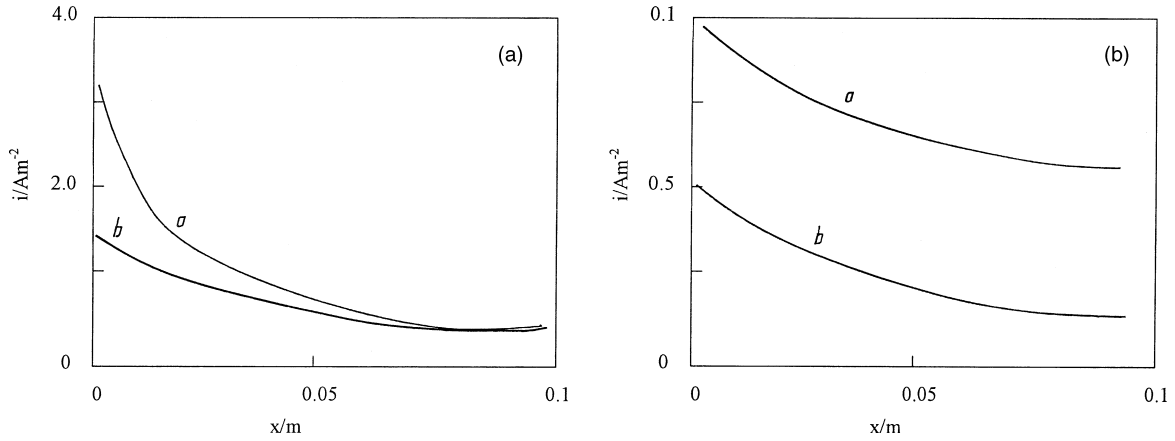

Fig. 5. (a) Variation in local overpotential and current density for the sparged packed bed reactor. (a) Current density: pH 13, $u_g = 0.1$ m s^{-1}, $u_l = 0.05$ m s^{-1}, $T = 298$ K, $d_p = 0.003$ m. Curves: *a* $\eta_o = 0.1$ V and *b* $\eta_o = 0.05$. (b) Overpotential: pH 13, $u_g = 0.1$ m s^{-1}, $u_l = 0.05$ m s^{-1}, $T = 298$ K, $d_p = 0.003$ m Curves: *a* $\eta_o = 0.1$ V and *b* $\eta_o = 0.05$ V.

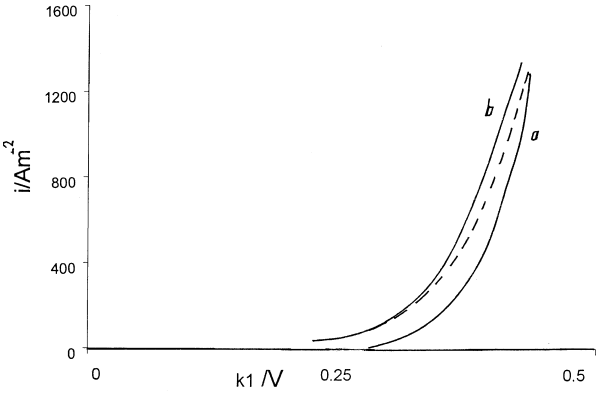

Fig. 6. Comparison of IOM predicted polarization behaviour with experimental data. (Conditions as in Tables 1 and 2). Curves: (*a*) literature values and (*b*) IOM values; (- - -) finite difference.

that using experimental literature data. The lack of agreement, especially at low overpotentials, reflects the difference in the electrochemical parameters determined in this work with those previously published and quoted in Table 2. This is confirmed from the inability of the model solution using finite difference to give good agreement with the literature values.

Table 3 compares the observed and predicted (IOM) potential, current behaviour of the reactor. Overall the data shows that the model predicts all of the experimental data points to within 20% and most of the data to within 10%. The greater deviation occurs at high overpotentials where the electrochemical side reaction, oxygen evolution, may be occurring.

Table 3. Observed, residual and predicted values of the model

Case	η/V	I_3 /A	$\hat{I}_3$/A	RES 3
1	0.05	0.050	0.040	0.010
2	0.10	0.150	0.110	0.040
3	0.15	0.230	0.220	0.010
4	0.20	0.330	0.350	−0.020
5	0.25	0.430	0.460	−0.030
6	0.30	0.500	0.540	−0.040
7	0.35	0.600	0.580	0.020
8	0.40	0.750	0.600	0.150
9	0.45	0.775	0.615	0.160

Figure 7 compares the predicted distributions in current density using finite differences routine BAND(J) and the IOM method. Agreement between the two is fairly good at low overpotential of <0.2 V. At higher overpotential agreement is still reasonable with values of current density within 10% of each other.

5. Conclusions

The inverse operator method, which is a technique for the approximate solution of nonlinear differential equations, is potentially useful in the study of electrochemical reaction engineering. IOM is a convenient method for studying the behaviour of the SPBER as it provides an approximate analytical solution of the model. From the analytical solution the relationship between the

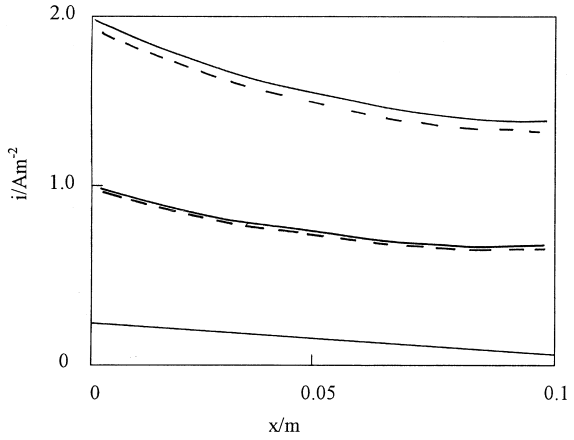

Fig. 7. Comparison of current density distributions using the finite difference solution and the IOM approximation. Values of overpotential at the diaphragm, $k_1 = 0.3$ V. $e_g = 0.16$, $\alpha = 0.35$, $i_o = 1.2 \times 10^4$ A m^{-2}, pH 13. Key: (—) IOM and (- - -) finite difference.

behaviour of SPBER and various parameter is clearer and is more easily tested by experiment. The analytical IOM model has been satisfactorily tested by experimental and regression results for the anodic oxidation of propylene to propylene oxide. The model predicts all the experimental data points to within 20% and most of the data to within 10%. The degree of accuracy obtained for the kinetic and mass transport parameters is considered suitable for engineering purposes. It has been demonstrated that the liquid–solid mass transport has an important influence on the process under experimental conditions. The gas sparging rate has a major impact on the reactor performance, and should be optimised in practice.

Appendix

Adomian [21, 22] developed the decomposition method to solve a wide range of non-linear differential equations in the late 1980s and 1990s. The method is capable of processing either determinative or random, either ordinary or partial, differential equations. The procedure is described here in relation to the problem concerned in this paper.

A.1. *The decomposition*

A differential equation may be expressed by an operator equation:

$$\tilde{F}y = \mathrm{g}(t) \tag{A1}$$

With the decomposition method the equation is decomposed in three ways. The first decomposition is for the operator, supposing it is determinative:

$$\tilde{F} = L + R + N \tag{A2}$$

L is a linear operator whose inverse plays a key part in the Adomian decomposition method. Although it can be chosen in different ways, its inverse operation must exist and be carried out without difficulty, which means that the related Green function should have an explicit form and be easy to obtain [21]. If choosing the highest differential operator as L, its inverse is common integration. R is the left linear operator and N is the nonlinear operator of the equation.

Substituting Equation A2 into Equation A1 and operating with the inverse operator L^{-1}, provides a way to obtain the solution:

$$L^{-1}Ly = L^{-1}\mathrm{g}(t) - L^{-1}Ry - L^{-1}Ny \tag{A3}$$

From this formula, it is seen that the decomposition method is still an indirect approach.

Secondly, the final solution is decomposed by a partial series, which should be convergent:

$$y = \sum_{n=0}^{\infty} y_n \tag{A4}$$

The third decomposition is for the nonlinear term Ny. Adomian [21] took a special polynomial series to approach the nonlinear term:

$$Ny = \sum_{n=0}^{\infty} A_n \tag{A5}$$

Each A_n is determined only by those partial solutions whose order is less than or equal to n.

Combining Equations A3, A4 and A5, the solution formulas are determined. The initial partial solution is

$$y_0 = L^{-1}\mathrm{g}(t) + \phi_0 \tag{A6}$$

The following partial solutions are obtained by iterations:

$$y_{n+1} = -L^{-1}Ry_n - L^{-1}A_n + \phi_{n+1} \tag{A7}$$

ϕ is determined by the initial or boundary conditions. So, by providing the necessary Adomian polynomials, obtaining the solutions could simply be made through routine calculations.

A.2. *Adomian polynomial*

Using power series to derive special polynomials to solve linear differential equations is a classic mathematical method, for example, Legendre polynomials and the Legendre equation. Adomian Polynomials are based on the same concept and are extended to nonlinear differential equations.

Supposing operator N as a nonlinear function $v(y)$, considering Taylor series of $v(y)$ about the centre y_0:

$$v(y) = v(y_0) + v'(y_0)(y - y_0) + \frac{1}{2!}v''(y_0)(y - y_0)^2 + \cdots \tag{A8}$$

From Equation A2 on substitution we obtain:

$$y - y_0 = y_1 + y_2 + \cdots$$

Technically transforming it with a parameter λ and an intentional differential operator, which helps a 'shooting' effect for partial solutions with a given order, we obtain:

$$\sum_{n=0}^{\infty} A_n = \sum_{n=0}^{\infty}\left[v(y_0)\frac{\mathrm{d}^n}{\mathrm{d}\lambda^n}\bigg|_{\lambda=0}\lambda^0 + v'(y_0)\frac{\mathrm{d}^n}{\mathrm{d}\lambda^n}\bigg|_{\lambda=0}(\lambda y_1 + \lambda^2 y_2 + \cdots) + \frac{1}{2!}v''(y_0)\frac{\mathrm{d}^n}{\mathrm{d}\lambda^n}\bigg|_{\lambda=0}(\lambda y_1 + \lambda^2 y_2 + \cdots)^2 + \cdots\right] \tag{A9}$$

Providing n with different integer values, Adomian polynomials with various orders are determined:

$$\begin{aligned} A_0 &= v(y_0) \\ A_0 &= v'(y_0)y_1 \\ A_2 &= v'(y_0)y_2 + \frac{1}{2!}v''(y_0)y_1^2 \\ A_3 &= v'(y_0)y_3 + v''(y_0)y_1y_2 + \frac{1}{3!}v'''(y_0)y_1^3 \end{aligned} \tag{A10}$$

For higher order Adomian polynomials the deduction becomes more complex, so Rach et al. (1984) [23] supplied rules for the deduction of Adomian polynomials. Of course, the solution convergent speed is a critical factor application of the decomposition method; fast convergence means only a few low order Adomian polynomials are necessary for the final solution.

References

1. K. Scott and Y.P. Sun, *Electrochim. Acta* **40** (4) (1995) 423.
2. C.R. Alkire and J.D. Lisius, *J. Electrochem. Soc.* **132** (1985) 1879.
3. K. Scott, C. Odouza and W. Hui, *Chem. Eng. Sci.* **47** (1992) 2957.
4. M.M. Baizer, 'Organic Electrochemistry' (Marcel Dekker, New York, 1973).
5. T.C. Chou and J.C. Chang, *Chem. Eng. Sci.* **35** (1980) 1581.
6. C.F. Odouza and K. Scott, *I Chem. E. Symp. Series* No. 127 (1992) 37.
7. J.S. Newman, 'Electrochemical Systems', (Prentice Hall, Englewood Cliffs, NJ, 1973).
8. G. Adomian, 'Stochastic Systems', (Academic Press, New York, 1983).
9. F. Jinqing and Y. Weiguang, *Wuli Xuebao* **42**(9) (1992) 1375.
10. D. Bennion, *A. I. Chem. E. Symposium Ser.* No. 229 (1983) 79.
11. I. Rousar, K. Micka and A. Kimla, 'Electrochemical Engineering' Vol. 1 (Elsevier Science, Amsterdam, 1986).
12. M.I. Ismail (Ed.), 'Electrochemical Reactors-Their Science and Technology, Part A Fundamentals, Electrolysers, Batteries and Fuel Cells' (Elsevier Science, Amsterdam, 1989), p. 135.
13. H. Hikita, S. Asai, K. Tanigawa, K. Segawa and M. Kitao, *Chem. Eng. J.* **20** (1980) 59.
14. V. Specchia, S. Sicardi and A. Gianetto, *A. I. Ch. E. J.* **20** (174) 646.
15. J.W. Snider and J.J. Perona, *A. I. Ch. E. J.* **20** (174) 1172.
16. C.Y.L. Wen and L.T. Fan, 'Models for Flow Systems and Chemical Reactors' (Marcel Dekker, New York, 1975), p. 187.
17. J. Van Zee and R.E. White, *J. Electrochem. Soc.* **130** (10) (1983) 2003.
18. Statistics for Windows, release 5.0, copyright Statsoft. Inc. 1984–1995, Tulsa USA.
19. S.F. Li, 'Chemical and Catalytic Reaction Engineering' (Chemical Industry Publications, Tian Jing, 1986).
20. K. Scott, *Electrochimi. Acta* **27** (1982) 447.
21. G. Adomian, 'Solving Frontier Problems of Physics: The Decomposition Method' (Kluwer Academic, Dordrecht 1994).
22. G. Adomian, 'A Summary of the Decomposition Method' Proceedings of Advances in Scientific Computing and Modelling' (Eastern Illinois University, Oct. 1996).
23. R. Rach, *J. Math. Analysis and Application* **102** (1984) 415.